JURNAL FARMASI SAINS DAN KOMUNITAS
Journal of Pharmaceutical Sciences & Community

p-ISSN 1693-5683; e-ISSN 2527-7146

Vol. 22, No. 2, November 2025, pp. 279-289

Research Article

Caffeine and Caffeic Acid as Acetylcholinesterase Inhibitors: In Silico Perspectives

Stephanus Satria Wira Waskitha[1], Bonifacius Ivan Wiranata[1,2], Julyus Jason Mark[1], Herluin Sekar Krisantia[1], Natalia Kristina[1], Glory Ivanna Ardine[1], Chrisologus Ivan Prasetyo[1], Michael Raharja Gani[1], Florentinus Dika Octa Riswanto[1], Enade Perdana Istyastono[1,3,*]

[1]Research Group of Computer-Aided Drug Design and Discovery of Bioactive Natural Products, Faculty of Pharmacy, Sanata Dharma University, Yogyakarta 55282, Indonesia
[2]Pharmaceutical Sciences Department, Faculty of Pharmacy, Widya Mandala Catholic University, Surabaya, Indonesia
[3]Departement of Pharmacy, Faculty of Medicine and Health Sciences, Atma Jaya Catholic University of Indonesia, Pluit Campus, Jl. Pluit Raya No. 2, Penjaringan, North Jakarta, DKI Jakarta 14440, Indonesia

https://doi.org/10.24071/jpsc.009687

J. Pharm. Sci. Community, 2025, 22(2), 279-289

Article Info

Received: 2024-09-02
Revised: 2024-10-22
Accepted: 2024-10-23

***Corresponding author:**
Enade Perdana Istyastono

email:
enade.istyastono@atmajaya.ac.id

Keywords:
Acetylcholinesterase; Alzheimer's disease; Caffeic acid; Caffeine; Molecular dynamics

ABSTRACT

Alzheimer's disease (AD) has been recognized as a significant issue affecting population health globally and tended to increase over the years. The utilization of natural products for AD treatments has been widely studied, which possibly offers better outcomes with minimum side effects. Coffee consumption has been subjected as a lifestyle propensity, which offers beneficial advantages including reducing the risk of AD. Bioactive natural compounds contained in coffee such as caffeine and caffeic acid have been experimentally proven to be acetylcholinesterase (AChE) inhibitors, a pivotal target enzyme for AD treatments. This research aimed to explore the dynamics interactions of caffeine and caffeic acid in the AChE active site using the in silico approach. In this study, 100 redocking and docking simulations were implemented before the molecular dynamics (MD) simulations. The 55-ns MD simulations of huprine X, caffeine, and caffeic acid were implemented to study the dynamics interactions. Conformational stability, free energies of binding, and interaction hotspots were identified during the simulations. Our findings informed that caffeine interacted in the active site during the simulations, revealing the importance of the imidazole ring in maintaining the interactions. In contrast, caffeic acid interacted longer in the plausible allosteric site, forming ionic, hydrogen bonds, and aromatic interactions.

INTRODUCTION

Alzheimer's disease (AD) is known as a neurodegenerative disorder characterized by gradual decline and dysfunction of cognitive and behavioral functions. This disease is also linked with dementia, the most prevalent type being AD. It was reported that 43.8 million people were suffering from dementia in 2016 (Nichols *et al.*, 2019). In fact, it was estimated that the prevalence would increase to 152.8 million cases in 2050 (Nichols *et al.*, 2022). Utilization of bioactive natural products has recently become a strategy to provide alternative treatments of AD (Bhat *et al.*, 2022). A wide range of plant extracts and bioactive natural compounds have been studied to give better treatment of AD with fewer side effects compared to the presently available treatments. Since AD depends on many causes, bioactive natural products provide substantial advantages, including multiple target selection of

distinguishable molecular sites in the human brain compared to the common AD drugs that have a single-target mechanism (Bhat *et al*., 2022).

Currently, coffee consumption has been highlighted as a lifestyle factor (Nila *et al*., 2023). Interestingly, recent studies showed that certain doses of coffee consumption reduced the risk of AD (Nila *et al*., 2023; Tira *et al*., 2023). Coffee also contains several bioactive natural compounds such as caffeine, caffeic acid, and other antioxidants (Akomolafe *et al*., 2017; Gani and Istyastono, 2021; Gobbi *et al*., 2023). Previous studies reported that caffeine and caffeic acid experimentally inhibited acetylcholinesterase (AChE), which is an enzyme that hydrolyzes acetylcholine into choline along with acetic acid and serves as a potential therapeutic target for treating AD (Akomolafe *et al*., 2017; Mohamed *et al*., 2013; Oboh *et al*., 2013). Our previous research also found that caffeic acid stably interacted in the AChE active site according to a molecular docking study (Waskitha *et al*., 2023). Nevertheless, as mentioned in the previous research, molecular docking results might be dubious, encouraging the researchers to validate the results with molecular dynamics (MD) simulations (Chen, 2015). As recently reported in our previous findings, the usefulness of PyPLIF HIPPOS 0.2.0 software could identify the prominent interactions formed from MD simulations results thereby providing us with the interaction hotspots (Istyastono *et al*., 2023; Istyastono and Riswanto, 2022).

This research aimed to study how caffeic acid and caffeine interact in the AChE active sites using in silico approaches. In this research, we conducted 100 molecular docking simulations followed by 55-ns MD simulations to evaluate the interaction stability. The results were further analyzed using PyPLIF HIPPOS 0.2.0. with its direct interactive fingerprinting (IFP) feature to identify the interaction hotspots throughout the simulations. This finding might hopefully provide in silico perceptions about the molecular mechanism of caffeic acid and caffeine in inhibiting the AChE enzyme.

METHODS

In Silico Instrumentations

A computer with central processing unit (CPU) specification of AMD Ryzen 7 5800X, graphics processing unit (GPU) of NVIDIA GeForce GTX 1650, 32 GB of random-access memory (RAM) along with 466 GB of solid-state drive (SSD) was used to perform all molecular simulations. This computer had the molecular simulation programs installed such as YASARA-Structure 24.4.10 embedded with our in-house developed plug-in for performing 100 redocking and molecular docking simulations. YASARA-Structure 24.4.10 was also used for molecular dynamics simulations while PyPLIF HIPPOS 0.2.0 was utilized for interaction hotspots identification (Istyastono *et al*., 2023).

Input File Preparation

The three-dimensional structure of acetylcholinesterase (AChE) complexed with its native ligand i.e., huprine X, was directly downloaded using YASARA-Structure with the Protein Data Bank (PDB) identification code of 1E66. The structure was manually corrected and prepared according to our previous research (Waskitha *et al*., 2023). This preparation included the addition of amino acids lost in the crystallographic structure, deletion of water molecules and the artifact residue (Nag), and terminal cap addition of the receptor, respectively. Further preparation was also conducted by correcting the native ligand structure, setting the system pH to 7.4 as the physiological condition, structure checking, and energy minimization. The prepared and corrected structure was then saved as 1e66-corr-min.yob for redocking simulations.

Redocking Simulations of Huprine X

The 100 redocking simulations of the native ligand were assisted using our in-house developed plug-in from our recent studies (Istyastono *et al*., 2023; Waskitha *et al*., 2023). This plug-in allowed us to automatically execute 100 redocking simulations with 1e66-corr-min.yob as the MacroTarget. These 100 redocking simulations resulted in redocking poses of the native ligand from the first to the last simulation. The root mean square deviation (RMSD) value of the best-docked pose of each simulation compared to the corrected crystallographic native ligand structure was also automatically calculated and the values were stored in a file named rmsd_bestpose_all.txt for redocking protocol validation (Diallo *et al*., 2021; Istyastono *et al*., 2023).

Molecular Docking Simulations of Caffeine and Caffeic Acid

These simulations were also executed using the same in-house developed plug-in from our recent studies (Istyastono *et al*., 2023; Waskitha *et al*., 2023). The 100 molecular docking simulations of caffeine and caffeic acid were performed separately in the different

working directories. The resulting files from the redocking simulations, i.e., MacroTarget_receptor.sce and MacroTarget_config.mcr were copied and then pasted into each working directory, allowing us to use the same molecular docking protocol as the redocking protocol. The three-dimensional structures of caffeine and caffeic acid were built using their SMILES codes, i.e., CN1C=NC2=C1C(=O)N(C(=O)N2C)C and C1=CC(=C(C=C1C=CC(=O)O)O)O, respectively. The system pH was adjusted to 7.4, thereby representing its structure in the physiological pH.

Each structure was automatically checked and energy minimized. The structure was then saved and used as the MacroTarget to perform 100 molecular docking simulations. Apart from the free energies of binding (FEB) calculated, the simulations resulted in RMSD values which compared the conformation and coordinate of the best-docked pose from each simulation to the best-docked pose from the first simulation. Accordingly, the best-docked compound from each simulation possessing RMSD value > 2.000 Å exhibits distinguishable conformation compared to the best-docked compound from the first simulation (Istyastono *et al*., 2023). As a result, the lower values of FEB indicated where the more stable interactions were formed.

Molecular Dynamics Simulations

The stability of the interactions formed from the molecular docking simulations was assessed using 55-ns molecular dynamics (MD) simulations. All MD simulations parameters were set in YASARA macro file i.e., md_run.mcr. The AMBER14 forcefield was selected to describe the forces between atoms and periodic boundary conditions were applied. A cube cell with a distance of 10 Å around all atoms was set with water molecules having a density of 0.993 g/mL in the system temperature and pressure of 310 K and 1 bar, respectively. In addition, Na+ and Cl- ions were added to the system with a concentration of 0.9%, depicting the physiological condition. Long-range coulomb forces were calculated using Particle Mesh Ewald with no cut off and the Van der Waals forces cut-off was set to 8.000 Å. Prior to the simulations, the steepest descent followed by simulated annealing energy minimizations were subjected to minimize steric hindrances in the system.

Eventually, 55-ns MD simulations were executed with a timestep of 2.5 fs, and the simulation snapshot was saved every 100 ps. In these simulations, the first 5 ns was regarded as the equilibration run followed by 10 ns of the production run to evaluate conformation stability at the initial production run. The production run was prolonged to 40 ns and therefore the production run took 50 ns with total simulations time of 55 ns. The simulations generated RMSD values of backbone atoms of the receptor (RMSD Backbone) and RMSD values of the ligand (RMSD Ligand Movement) in every saved snapshot. The alterations of RMSD values were used to access the conformational stability (Istyastono *et al*., 2023).

Free Energies of Binding (FEB) Analysis

The FEB of each MD simulations snapshot were calculated using YASARA-Structure macro file i.e., md_analyzebindingenergy.mcr. In the macro file, the AMBER14 force field was selected, adapting the consistency of the selected force field from the MD simulations. The solvation energy calculation was performed using Poisson-Boltzmann (PBS) at the temperature of 310 K. Finally, the FEB were calculated using the VINA local search (VINALS) algorithm.

Interaction Hotspots Identification

Interaction hotspot identification was executed using PyPLIF HIPPOS 0.2.0. with its direct IFP feature as recently used in our previous research (Istyastono *et al*., 2023). All MD simulations snapshots were converted into pdb format using YASARA macro file i.e., md_convert.mcr without water molecules contained in the system. All interactions defined by PyPLIF HIPPOS 0.2.0. from each MD simulations snapshot were clustered according to the interaction type to identify the interaction hotspots throughout 55-ns MD simulations.

RESULTS AND DISCUSSION

Molecular Docking Simulations Targeting Acetylcholinesterase (AChE)

Initially, redocking simulations of the native ligand were executed before performing molecular docking simulations of both caffeine and caffeic acid targeting the AChE active site. Aside from understanding the native ligand interactions formed, redocking simulations aimed to evaluate the reliability and validity of the proposed redocking protocol (Diallo *et al*., 2021; Istyastono *et al*., 2023). The 100 redocking simulations resulted in stable conformation of the best-docked poses, exhibiting an average FEB of -13.119 kcal/mol. Therewith, 100 redocking simulations generated the best-docked poses having RMSD value ≤ 2.000 Å compared to the corrected crystallographic native ligand

conformation. These results indicated that the redocking protocol was considerably valid and could be used for further processes, i.e., molecular docking of caffeine and caffeic acid, separately (Diallo *et al*., 2021; Istyastono *et al*., 2023). The lowest RMSD value was 0.207 Å, possessing FEB of -13.115 kcal/mol which was closely similar to the average FEB value. The conformation stability of this best-docked pose was evaluated with 55-ns MD simulations as this conformation was the most closely resembling the crystallographic conformation.

Molecular docking simulations of caffeine resulted in all the best-docked poses possessing RMSD value of ≤ 2.000 Å compared to the best-docked pose of the first simulation. This result pointed out that there was only one best-docked caffeine conformation dominantly, which possessed an average FEB of -7.009 kcal/mol. The lowest FEB was -7.032 kcal/mol, forming interactions with amino acid residues of the active site such as Tyr70, Asp72, Trp84, Gly118, Tyr121, Ser122, Phe330, Tyr334, Trp432, and Tyr442 along with two of three catalytic triad residues i.e., Ser200 and His440. Interestingly, molecular docking simulations of caffeic acid in the AChE active site resulted in a difference compared to caffeine. These simulations produced 95 out of 100 of the best-docked conformations with RMSD value of ≤ 2.000 Å, thereby generating two probabilities of the best-docked conformations. As we analyzed the FEB, the dominant best-docked poses possessed an average FEB of -7.931 kcal/mol whereas the rest possessed a relatively close average FEB of -7.940 kcal/mol. The lowest FEB of the best-docked caffeic acid was -7.968 kcal/mol, which was also representing the dominant best-docked poses. This best-docked pose was stabilized with amino acid residues of the active site as the lowest FEB of the best-docked caffeine interacted. In this research, to evaluate the interaction stability of the lowest FEB of the best-docked caffeine and caffeic acid, molecular dynamics (MD) simulations were executed to validate the molecular docking simulations results.

Molecular Dynamics (MD) Simulations

The conformational stability of AChE backbone atoms and the docked ligands was assessed using MD simulations, as depicted in Figures 1 and 2, respectively. A conformation is considered stable if the RMSD value is ≤ 2.000 Å compared to the reference structure (Liu and Kokubo, 2017). As seen in Figure 1, the RMSD value of backbone atoms of AChE complexed with huprine X remained stable in the equilibration run, i.e., until 4.9 ns. Afterward, the RMSD backbone value increased gradually with RMSD backbone value of 2.896 Å at 6.8 ns. Even though there were decreasing RMSD backbone values until 8.4 ns, the value once escalated to 2.899 Å at 9.7 ns then remained relatively steady until 46.9 ns. Thereafter, the RMSD backbone value tended to decrease until the end of the simulations. Excitingly, the RMSD ligand movement of huprine X remained stable with relatively low alterations of the RMSD value, retaining RMSD values ≤ 2.000 Å throughout simulations (Figure 2). These considerably steady conformations were due to intermolecular interactions of the AChE active site such as the hydrogen bonds and aromatic interactions as tabulated in Table 1.

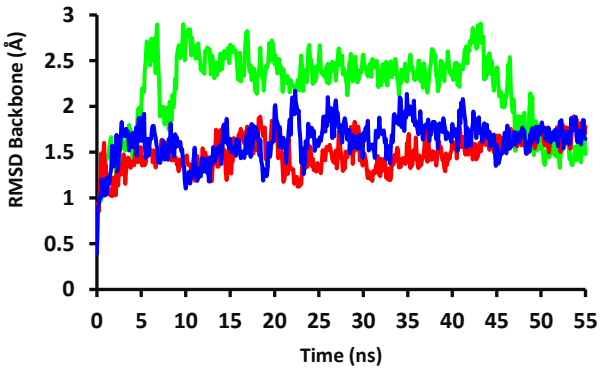


Figure 1. The alteration of RMSD backbone atoms value of AChE complexed with huprine X (green), caffeine (red), and caffeic acid (blue) throughout 55-ns MD simulations

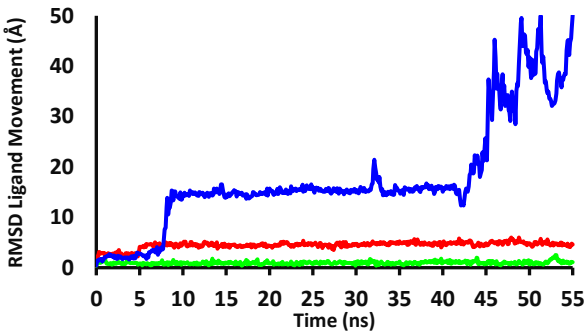


Figure 2. The alteration of RMSD Ligand Movement value of huprine X (green), caffeine (red), and caffeic acid (blue) throughout 55-ns MD simulations.

Table 1. Non-hydrophobic interactions hotspots identified by PyPLIF HIPPOS 0.2.0 calculating interacting residues of AChE-huprine X throughout 55-ns MD simulations

Interacting Residue	Interaction Type	Interaction Percentage
Trp84	Aromatic face-to-face	92.74 %
	Aromatic edge-to-face	59.52 %
Tyr121	Aromatic edge-to-face	0.18 %
Phe330	Aromatic face-to-face	95.82 %
	Aromatic edge-to-face	21.23 %
Tyr334	Aromatic edge-to-face	66.42 %
Trp432	Aromatic face-to-face	24.13 %
	Aromatic edge-to-face	72.95 %
His440	Aromatic face-to-face	6.35 %
	Aromatic edge-to-face	23.23 %
Tyr442	Aromatic face-to-face	0.36 %
	Aromatic edge-to-face	73.86 %
	H-bond donor	2.17 %

In the MD simulations, PyPLIF HIPPOS 0.2.0 identified receptor-ligand interactions formed such as ionic, hydrogen bond, aromatic, and hydrophobic interactions. Nevertheless, this research exposed only non-hydrophobic interactions, i.e., ionic, hydrogen bond, and aromatic interactions since all amino acid residues of the AChE active site could form hydrophobic interactions especially with the hydrophobic moiety of the ligand as observed in the previous research (Windah and Istyastono, 2024). Our findings indicated that PyPLIF HIPPOS 0.2.0 identified amino acid residues of the active site such as Trp84, Tyr121, Phe330, Tyr334, and other amino acid residues tabulated in Table 1. This research revealed that the nitrogen atom of 4-aminopyridine moiety formed hydrogen bonds with Tyr442 at several MD simulations snapshots. In addition, amino acid residues of Trp84, Phe330, Tyr334, Trp432, and Tyr442 formed aromatic interactions with aromatic moiety of huprine X more than 50% during the 55-ns simulations.

These results were also in good correlation with the previous research, revealing that 4-aminopyridine moiety had a crucial role in stabilizing interactions in the AChE active site as well as maintaining the inhibitory activity (Ronco *et al*., 2011; Sinha and Shrivastava, 2013). Indeed, these simulations also might explain the molecular interactions of huprine X as an AChE inhibitor experimentally reported by the previous research (Luque and Muñoz-Torrero, 2024; Relat *et al*., 2018; Ziemianin *et al*., 2012). As exhibited in Figure 3, the FEB of huprine X throughout the simulations were comparably lower than caffeine and caffeic acid as well, denoting the more stable interactions. Nevertheless, there were increasing FEB at 3.7, 19.0, and 49.6 ns severally which might be due to unfavorable steric bumping interactions or weaker interactions formed.

Although the conformational backbone atoms stability of AChE complexed with huprine X was relatively altered and noticeably unstable at mostly several snapshots, the conformational

backbone atoms stability of AChE complexed with caffeine and caffeic acid was comparatively more stable as depicted in Figure 1.

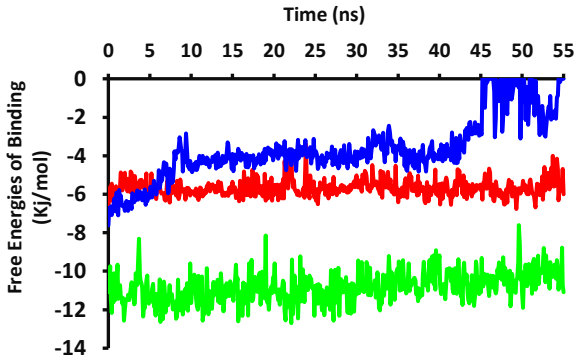


Figure 3. The free energies of binding resulted from each MD simulations snapshot reflecting interactions of huprine X (green), caffeine (red), and caffeic acid (blue) with amino acid residues of AChE.

Table 2. Non-hydrophobic interactions hotspots identified by PyPLIF HIPPOS 0.2.0 calculating interacting residues of AChE-caffeine throughout 55-ns MD simulations

Interacting Residue	Interaction Type	Interaction Percentage
Ser81	H-bond donor	0.90 %
Trp84	H-bond donor	0.18 %
	Aromatic face-to-face	93.28 %
	Aromatic edge-to-face	1.08 %
Asn85	H-bond donor	0.18 %
Tyr130	H-bond donor	0.18 %
Phe330	Aromatic face-to-face	13.61 %
	Aromatic edge-to-face	72.41 %
Phe331	Aromatic face-to-face	0.18 %
Tyr334	Aromatic edge-to-face	2.17 %
Trp432	Aromatic face-to-face	42.10 %
	Aromatic edge-to-face	37.56 %
His440	Aromatic face-to-face	0.90 %
	Aromatic edge-to-face	1.99 %
Tyr442	H-bond donor	0.54 %
	H-bond acceptor	0.90 %
	Aromatic edge-to-face	83.48 %

Interestingly, AChE complexed with caffeine retained conformational backbone atoms of the receptor stably, with RMSD value ≤ 2.000 Å during 55-ns simulations. It could be observed that caffeine has RMSD ligand movement values of more than 2.000 Å at the initial equilibration run (0.1 ns) until the end of the simulations, as shown in Figure 2. At the equilibration run of 0.1 to 4.9 ns, the highest RMSD resulted was 3.506 Å. Yet, caffeine still interacted in the AChE active site as shown by contribution of hydrogen bonds formation with Tyr130 and aromatic interactions with amino acid residues of Trp84, Phe330, Phe331, His440, and Tyr442.

Starting from the end of the equilibration run (5.0 ns) until the end of simulations, the RMSD ligand movement of caffeine was in the range of 3.507 – 5.992 Å. At this simulation time range, caffeine was unpredictably still in the AChE active site forming several hydrogen bonds with amino acid residues of Ser81, Trp84, Asn85, and Tyr442 at several snapshots, along with other interactions such as aromatic interactions with Trp84, Phe330, Tyr334, Trp432, and Tyr442. Our visual inspection revealed the importance of the nitrogen atom in the imidazole ring and the carbonyl moiety of caffeine to stabilize the interactions via hydrogen bond formation with these amino acid residues. The FEB of caffeine, as graphically depicted in Figure 3, also confirmed that the interactions formed were energetically stable compared to the FEB of

huprine X though the values were higher. This FEB resulted were caused by several interactions especially hydrogen bonds and aromatic interactions during the simulations as shown in Table 2. As expected, the primary interactions formed due to the imidazole ring of caffeine. Besides the hydrogen bonds formed, the imidazole ring formed aromatic interactions predominantly with Trp84, Phe330, and Tyr442 throughout the simulations. This imidazole ring feature was also observed in bioactive natural compounds inhibiting AChE such as xanthine, theobromine, and theophylline as mentioned in the previous research (Reshetnikov *et al*., 2022). These interactions, especially the aromatic interactions, were also observed in the huprine X interactions, representing the importance of heteroaromatic ring moiety to stabilize the interactions in the AChE active site.

As perceived in Figure 1, backbone atoms of AChE complexed with caffeic acid tended to be more stable compared to huprine X even though there were RMSD value fluctuations exceeding 2.000 Å at several MD snapshots, with the highest value of 2.172 Å. Caffeic acid retained interactions stably at the initial equilibration run, i.e., until 0.9 ns then the RMSD ligand movement value tended to increase gradually until 8.0 ns with a maximum RMSD ligand movement value of 7.888 Å. At the equilibration run until the early production run, from 0.0 to 8.0 ns, caffeic acid still formed interactions in the AChE active site, forming interactions of hydrogen bonds along with aromatic interactions as tabulated in Supplementary File 1. The formed interactions along this simulation time might be considerably weaker interactions since there was a tendency to increase FEB as graphically shown in Figure 3.

Figure 3 shows that there were fluctuating FEB from 8.0 to 8.7 ns as caffeic acid started escaping the AChE active site, showing highly increasing values in the RMSD ligand movement notably starting from 7.6 ns. The RMSD ligand movement value reached 15.332 Å at 8.7 ns with no interactions with amino acid residues of the AChE active site, forming hydrophobic interactions with amino acid residues of Met83 and Leu456 in the plausible allosteric site. Starting from 8.7 to 44.9 ns, caffeic acid formed interactions in the plausible allosteric site though there were highly fluctuating RMSD ligand movement values from 32.0 to 32.2 ns along with decreasing values from 41.9 ns to 42.4 ns followed by increasing values until 44.9 ns. In this allosteric site, caffeic acid was stabilized by ionic interactions with Lys133 (5.23%) and several hydrogen bonds interactions, especially with Glu445 (62.53%) along with aromatic (edge-to-face) interactions with Trp84 (0.28%) as tabulated in Table 3.

At 45.0 ns, caffeic acid moved freely escaping the receptor and interacting with water molecules. It could be observed that there were several FEB of 0.000 kJ/mol, indicating that caffeic acid no longer interacted with any amino acid residues of AChE in several snapshots ranging from 45 to 55 ns of the simulations, as shown in Figure 3. Nevertheless, caffeic acid tended to reach any amino acid residues in the outer AChE enzymes, i.e., Lys270, Lys52, Gln162, Glu229 at several snapshots at the end of the simulations. All formed interactions of caffeic acid identified by PyPLIF HIPPOS 0.2.0 along 55-ns MD simulations were tabulated in Supplementary File 2. According to the results, caffeic acid interacted unstably in the AChE active site and tended to occupy a plausible allosteric site even though it also was proved to escape the receptor interactions at the end of the simulations. Hence, our findings might suggest caffeic acid was a non-competitive inhibitor as other non-competitive AChE inhibitors, i.e., bromotyrosine alkaloids (Olatunji *et al*., 2014), tacrine (Bai *et al*., 2000), certain flavonoids (Khan *et al*., 2018; Remya *et al*., 2012) and also peptides (Asen *et al*., 2022) as previously reported.

Table 3. Non-hydrophobic interactions hotspots identified by PyPLIF HIPPOS 0.2.0 calculating interacting residues of AChE-caffeic acid in the plausible allosteric site throughout 8.7 to 44.9 ns MD simulations

Interacting Residue	Interaction Type	Interaction Percentage
Trp84	Aromatic edge-to-face	0.28%
Lys133	H-bond donor	2.75%
	Ionic as the cation	5.23%
Tyr134	H-bond donor	1.38%
Tyr442	H-bond acceptor	0.55%
	H-bond donor	1.38%
Glu445	H-bond acceptor	62.53%
Tyr458	H-bond donor	0.55%

As supposed, caffeic acid was stabilized by ionic, hydrogen bonds, and aromatic interactions in the plausible allosteric site, denoting the importance of the hydroxyl, aromatic, and carboxyl moiety of caffeic acid according to this study. These features were in parallel with the previous research reported, which denoted that the hydroxyl and aromatic moiety of caffeic acid phenethyl ester derivatives might increase the inhibitory activity of AChE (Gießel *et al*., 2019). Also, another research reported the pivotal role of carboxyl group in inhibiting AChE (Santos and Takahashi, 2017). Furthermore, the allosteric site identified by these MD simulations could provide validation for compounds resembling caffeic acid structure, i.e., cinnamic acid and ferulic acid or their derivatives as mentioned in the previous research (Saeed *et al*., 2014; Zhang *et al*., 2018), informing the importance of the moiety of those compounds as AChE inhibitors.

Recapping the key points, caffeine still interacted in the AChE active site during the MD simulations while caffeic acid tended to bind in the plausible allosteric site and then managed to escape the receptor at the end of the simulations. The results denoted that caffeine possessed a better affinity to the receptor than caffeic acid. Our results might explain and were well-matched with the previous research, showing that caffeine had a better inhibitory inhibition of AChE (IC_{50} = 7.25 µM) than caffeic acid (IC_{50} = 4.21 µg/mL or 23.36 µM) (Mohamed *et al*., 2013; Oboh *et al*., 2013) identified using the Ellman method. Hence, a possible explanation for the weaker inhibitory effect of caffeic acid compared to caffeine could be its tendency to leave the receptor more easily.

The capacity of drugs to penetrate the blood-brain barrier (BBB) is a critical factor when developing treatments for neurodegenerative disorders (Li *et al*., 2015). Remarkably, previous studies also denoted that caffeine and caffeic acid were able to cross the BBB, indicating the good expectancy of these compounds as AChE inhibitors (Grabska-Kobylecka *et al*., 2020; McCall *et al*., 1982; Ren and Chen, 2020; Ruggiero *et al*., 2022). Therefore, developing effective treatments for Alzheimer's disease should take into account the ability of potential drugs to penetrate the BBB as many other common AChE inhibitors (Pohanka, 2014).

CONCLUSIONS

Molecular dynamics simulations revealed huprine X and caffeine interacted in the AChE active site throughout the simulations. Our findings found that huprine X and caffeine interactions were reinforced by the hydrogen bonds and aromatic interactions, which also signified the importance of the aromatic ring for ligand-receptor stabilization. Caffeic acid noticeably interacted in the AChE active at the initial stage of the simulations then occupied the plausible allosteric site and finally escaped the receptor at the end of the simulations. Our contrivance hopefully could be used to comprehend the molecular level of bioactive compounds contained in coffee, i.e., caffeine and caffeic acid in inhibiting the AChE enzyme according to in silico perspectives.

ACKNOWLEDGEMENTS

This research was granted by Lembaga Penelitian dan Pengabdian Kepada Masyarakat Universitas Sanata Dharma (LPPM USD) (Research Grant Contract No.: 019 PeneI./LPPM-USD/III/2024).

CONFLICT OF INTEREST

The authors declare no conflict of interest.

REFERENCES

Akomolafe, S.F., Akinyemi, A.J., Ogunsuyi, O.B., Oyeleye, S.I., Oboh, G., Adeoyo, O.O., Allismith, Y.R., 2017. Effect of caffeine, caffeic acid and their various combinations on enzymes of cholinergic, monoaminergic and purinergic systems critical to neurodegeneration in rat brain—in vitro. *NeuroToxicology,* 62, 6–13.

Asen, N.D., Okagu, O.D., Udenigwe, C.C., Aluko, R.E., 2022. In vitro inhibition of acetylcholinesterase activity by yellow field pea (Pisum sativum) protein-derived peptides as revealed by kinetics and molecular docking. *Frontiers in Nutrition,* 9(1021893), 1–18.

Bai, D.L., Tang, X.C., He, X.C., 2000. Huperzine A, a potential therapeutic agent for treatment of Alzheimer's disease. *Current Medicinal Chemistry,* 7(3), 355–374.

Bhat, B.A., Almilaibary, A., Mir, R.A., Aljarallah, B.M., Mir, W.R., Ahmad, F., Mir, M.A., 2022. Natural therapeutics in aid of treating Alzheimer's disease: A green gateway

toward ending quest for treating neurological disorders. *Frontiers in Neuroscience*, 16(884345), 1–23.

Chen, Y.C., 2015. Beware of docking! *Trends in Pharmacological Sciences,* 36(2), 78–95.

Diallo, B.N., Swart, T., Hoppe, H.C., Tastan Bishop, Ö., Lobb, K., 2021. Potential repurposing of four FDA approved compounds with antiplasmodial activity identified through proteome scale computational drug discovery and in vitro assay. *Scientific Reports,* 11(1), 1–15.

Gani, M.R., Istyastono, E.P., 2021. Determination of caffeic acid in ethanolic extract of spent coffee grounds by high-performance liquid chromatography with UV detection. Indonesian *Journal of Chemistry,* 21(5), 1281–1286.

Gießel, J.M., Loesche, A., Csuk, R., 2019. Caffeic acid phenethyl ester (CAPE)-derivatives act as selective inhibitors of acetylcholinesterase. *European Journal of Medicinal Chemistry*, 177, 259–268.

Gobbi, L., Maddaloni, L., Prencipe, S.A., Vinci, G., 2023. Bioactive compounds in different coffee beverages for quality and sustainability assessment. *Beverages,* 9(1), 1–18.

Grabska-Kobylecka, I., Kaczmarek-Bak, J., Malgorzata, F., Prymont-Przyminska, A., Zwolinska, A., Sarniak, A., Wlodarczyk, A., Glabinski, A., Nowak, D., 2020. The presence of caffeic acid in cerebrospinal fluid: Evidence that dietary polyphenols can cross the blood-brain barrier in humans. *Nutrients*, 12(5), 1531.

Istyastono, E.P., Riswanto, F.D.O., 2022. Molecular dynamics simulations of the caffeic acid interactions to dipeptidyl peptidase IV. *International Journal of Applied Pharmaceutics*, 14(4), 274–278.

Istyastono, E.P., Yuniarti, N., Prasasty, V.D., Mungkasi, S., Waskitha, S.S.W., Yanuar, M.R.S., Riswanto, F.D.O., 2023. Caffeic acid in spent coffee grounds as a dual inhibitor for MMP-9 and DPP-4 enzymes. *Molecules*, 28(20), 1–12.

Khan, H., Marya, Amin, S., Kamal, M.A., Patel, S., 2018. Flavonoids as acetylcholinesterase inhibitors: Current therapeutic standing and future prospects. *Biomedicine and Pharmacotherapy*, 101, 860–870.

Li, H., Ye, M., Zhang, Y., Huang, M., Xu, W., Chu, K., Chen, L., Que, J., 2015. Blood-brain barrier permeability of Gualou Guizhi granules and neuroprotective effects in ischemia/reperfusion injury. *Molecular Medicine Reports,* 12(1), 1272–1278.

Liu, K., Kokubo, H., 2017. Exploring the stability of ligand binding modes to proteins by molecular dynamics simulations: A cross-docking study. *Journal of Chemical Information and Modeling,* 57(10), 2514–2522.

Luque, F.J., Muñoz-Torrero, D., 2024. Acetylcholinesterase: a versatile template to coin potent modulators of multiple therapeutic targets. *Accounts of Chemical Research,* 57, 450–456.

McCall, A.L., Millington, W.R., Wurtman, R.J., 1982. Blood-brain barrier transport of caffeine: Dose-related restriction of adenine transport. *Life Sciences,* 31(24), 2709–2715.

Mohamed, T., Osman, W., Tin, G., Rao, P.P.N., 2013. Selective inhibition of human acetylcholinesterase by xanthine derivatives: In vitro inhibition and molecular modeling investigations. *Bioorganic and Medicinal Chemistry Letters*, 23(15), 4336–4341.

Nichols, E., Steinmetz, J.D., Vollset, S.E., Fukutaki, K., Chalek, J., Abd-Allah, F., Abdoli, A., Abualhasan, A., Abu-Gharbieh, E., Akram, T.T., Al Hamad, H., Alahdab, F., Alanezi, F.M., Alipour, V., Almustanyir, S., Amu, H., Ansari, I., Arabloo, J., Ashraf, T., Astell-Burt, T., Ayano, G., Ayuso-Mateos, J.L., Baig, A.A., Barnett, A., Barrow, A., Baune, B.T., Béjot, Y., Mequanint Bezabhe, W.M., Bezabih, Y.M., Bhagavathula, A.S., Bhaskar, S., Bhattacharyya, K., Bijani, A., Biswas, A., Bolla, S.R., Boloor, A., Brayne, C., Brenner, H., Burkart, K., Burns, R.A., Cámera, L.A., Cao, C., Carvalho, F., Castro-De-Araujo, L.F.S., Catalá-López, F., Cerin, E., Chavan, P.P., Cherbuin, N., Chu, D.T., Costa, V.M., Couto, R.A.S., Dadras, O., Dai, X., Dandona, L., Dandona, R., De la Cruz-Góngora, V., Dhamnetiya, D., da Silva, D.D., Diaz, D., Douiri, A., Edvardsson, D., Ekholuenetale, M., El Sayed, I., El-Jaafary, S.I., Eskandari, K., Eskandarieh, S., Esmaeilnejad, S., Fares, J., Faro, A., Farooque, U., Feigin, V.L., Feng, X., Fereshtehnejad, S.M., Fernandes, E., Ferrara, P., Filip, I., Fillit, H., Fischer, F., Gaidhane, S., Galluzzo, L., Ghashghaee, A., Ghith, N., Gialluisi, A., Gilani, S.A., Glavan, I.R., Gnedovskaya, E. V., Golechha, M., Gupta, R., Gupta, V.B., Gupta, V.K., Haider, M.R., Hall, B.J., Hamidi, S., Hanif, A., Hankey, G.J., Haque, S., Hartono, R.K., Hasaballah, A.I., Hasan, M.T., Hassan, A., Hay, S.I., Hayat, K., Hegazy, M.I., Heidari, G.,

Heidari-Soureshjani, R., Herteliu, C., Househ, M., Hussain, R., Hwang, B.F., Iacoviello, L., Iavicoli, I., Ilesanmi, O.S., Ilic, I.M., Ilic, M.D., Irvani, S.S.N., Iso, H., Iwagami, M., Jabbarinejad, R., Jacob, L., Jain, V., Jayapal, S.K., Jayawardena, R., Jha, R.P., Jonas, J.B., Joseph, N., Kalani, R., Kandel, A., Kandel, H., Karch, A., Kasa, A.S., Kassie, G.M., Keshavarz, P., Khan, M.A.B., Khatib, M.N., Khoja, T.A.M., Khubchandani, J., Kim, M.S., Kim, Y.J., Kisa, A., Kisa, S., Kivimäki, M., Koroshetz, W.J., Koyanagi, A., Kumar, G.A., Kumar, M., Lak, H.M., Leonardi, M., Li, B., Lim, S.S., Liu, X., Liu, Y., Logroscino, G., Lorkowski, S., Lucchetti, G., Saute, R.L., Magnani, F.G., Malik, A.A., Massano, J., Mehndiratta, M.M., Menezes, R.G., Meretoja, A., Mohajer, B., Ibrahim, N.M., Mohammad, Y., Mohammed, A., Mokdad, A.H., Mondello, S., Moni, M.A., Moniruzzaman, M., Mossie, T.B., Nagel, G., Naveed, M., Nayak, V.C., Kandel, S.N., Nguyen, T.H., Oancea, B., Otstavnov, N., Otstavnov, S.S., Owolabi, M.O., Panda-Jonas, S., Kan, F.P., Pasovic, M., Patel, U.K., Pathak, M., Peres, M.F.P., Perianayagam, A., Peterson, C.B., Phillips, M.R., Pinheiro, M., Piradov, M.A., Pond, C.D., Potashman, M.H., Pottoo, F.H., Prada, S.I., Radfar, A., Raggi, A., Rahim, F., Rahman, M., Ram, P., Ranasinghe, P., Rawaf, D.L., Rawaf, S., Rezaei, N., Rezapour, A., Robinson, S.R., Romoli, M., Roshandel, G., Sahathevan, R., Sahebkar, A., Sahraian, M.A., Sathian, B., Sattin, D., Sawhney, M., Saylan, M., Schiavolin, S., Seylani, A., Sha, F., Shaikh, M.A., Shaji, K.S., Shannawaz, M., Shetty, J.K., Shigematsu, M., Shin, J. Il, Shiri, R., Santos Silva, D.A., Silva, J.P., Silva, R., Singh, J.A., Skryabin, V.Y., Skryabina, A.A., Smith, A.E., Soshnikov, S., Spurlock, E.E., Stein, D.J., Sun, J., Tabarés-Seisdedos, R., Thakur, B., Timalsina, B., Tovani-Palone, M.R., Tran, B.X., Tsegaye, G.W., Tahbaz, S.V., Valdez, P.R., Venketasubramanian, N., Vlassov, V., Vu, G.T., Vu, L.G., Wang, Y.P., Wimo, A., Winkler, A.S., Yadav, L., Jabbari, S.H.Y., Yamagishi, K., Yang, L., Yano, Y., Yonemoto, N., Yu, C., Yunusa, I., Zadey, S., Zastrozhin, M.S., Zastrozhina, A., Zhang, Z.J., Murray, C.J.L., Vos, T., 2022. Estimation of the global prevalence of dementia in 2019 and forecasted prevalence in 2050: An analysis for the Global Burden of Disease Study 2019. *The Lancet Public Health*, 7(2), e105–e125.

Nichols, E., Szoeke, C.E.I., Vollset, S.E., Abbasi, N., Abd-Allah, F., Abdela, J., Aichour, M.T.E., Akinyemi, R.O., Alahdab, F., Asgedom, S.W., Awasthi, A., Barker-Collo, S.L., Baune, B.T., Béjot, Y., Belachew, A.B., Bennett, D.A., Biadgo, B., Bijani, A., Bin Sayeed, M.S., Brayne, C., Carpenter, D.O., Carvalho, F., Catalá-López, F., Cerin, E., Choi, J.Y.J., Dang, A.K., Degefa, M.G., Djalalinia, S., Dubey, M., Duken, E.E., Edvardsson, D., Endres, M., Eskandarieh, S., Faro, A., Farzadfar, F., Fereshtehnejad, S.M., Fernandes, E., Filip, I., Fischer, F., Gebre, A.K., Geremew, D., Ghasemi-Kasman, M., Gnedovskaya, E. V., Gupta, R., Hachinski, V., Hagos, T.B., Hamidi, S., Hankey, G.J., Haro, J.M., Hay, S.I., Irvani, S.S.N., Jha, R.P., Jonas, J.B., Kalani, R., Karch, A., Kasaeian, A., Khader, Y.S., Khalil, I.A., Khan, E.A., Khanna, T., Khoja, T.A.M., Khubchandani, J., Kisa, A., Kissimova-Skarbek, K., Kivimäki, M., Koyanagi, A., Krohn, K.J., Logroscino, G., Lorkowski, S., Majdan, M., Malekzadeh, R., März, W., Massano, J., Mengistu, G., Meretoja, A., Mohammadi, M., Mohammadi-Khanaposhtani, M., Mokdad, A.H., Mondello, S., Moradi, G., Nagel, G., Naghavi, M., Naik, G., Nguyen, L.H., Nguyen, T.H., Nirayo, Y.L., Nixon, M.R., Ofori-Asenso, R., Ogbo, F.A., Olagunju, A.T., Owolabi, M.O., Panda-Jonas, S., Passos, V.M. d. A., Pereira, D.M., Pinilla-Monsalve, G.D., Piradov, M.A., Pond, C.D., Poustchi, H., Qorbani, M., Radfar, A., Reiner, R.C., Robinson, S.R., Roshandel, G., Rostami, A., Russ, T.C., Sachdev, P.S., Safari, H., Safiri, S., Sahathevan, R., Salimi, Y., Satpathy, M., Sawhney, M., Saylan, M., Sepanlou, S.G., Shafieesabet, A., Shaikh, M.A., Sahraian, M.A., Shigematsu, M., Shiri, R., Shiue, I., Silva, J.P., Smith, M., Sobhani, S., Stein, D.J., Tabarés-Seisdedos, R., Tovani-Palone, M.R., Tran, B.X., Tran, T.T., Tsegay, A.T., Ullah, I., Venketasubramanian, N., Vlassov, V., Wang, Y.P., Weiss, J., Westerman, R., Wijeratne, T., Wyper, G.M.A., Yano, Y., Yimer, E.M., Yonemoto, N., Yousefifard, M., Zaidi, Z., Zare, Z., Vos, T., Feigin, V.L., Murray, C.J.L., 2019. Global, regional, and national burden of Alzheimer's disease and other dementias, 1990–2016: A systematic analysis for the Global Burden of Disease Study 2016. *The Lancet Neurology,* 18(1), 88–106.

Nila, I.S., Villagra Moran, V.M., Khan, Z.A., Hong, Y., 2023. Effect of daily coffee consumption on the risk of Alzheimer's disease: A systematic review and meta-analysis.

Journal of Lifestyle Medicine, 13(2), 83–89.

Oboh, G., Agunloye, O.M., Akinyemi, A.J., Ademiluyi, A.O., Adefegha, S.A., 2013. Comparative study on the inhibitory effect of caffeic and chlorogenic acids on key enzymes linked to Alzheimer's disease and some pro-oxidant induced oxidative stress in rats' brain-in vitro. *Neurochemical Research*, 38(2), 413–419.

Olatunji, O.J., Ogundajo, A.L., Oladosu, I.A., Changwichit, K., Ingkaninan, K., Yuenyongsawad, S., Plubrukarn, A., 2014. Non-competitive inhibition of acetylcholinesterase by bromotyrosine alkaloids. *Natural Product Communications,* 9(11), 1559–1561.

Pohanka, M., 2014. Inhibitors of acetylcholinesterase and butyrylcholinesterase meet immunity. International *Journal of Molecular Sciences,* 15(6), 9809–9825.

Relat, J., Pérez, B., Camps, P., Muñoz-Torrero, D., Badia, A., Victòria Clos, M., 2018. Huprine X attenuates the neurotoxicity induced by kainic acid, especially brain inflammation. *Basic and Clinical Pharmacology and Toxicology,* 122(1), 94–103.

Remya, C., Dileep, K. V., Tintu, I., Variyar, E.J., Sadasivan, C., 2012. Design of potent inhibitors of acetylcholinesterase using morin as the starting compound. *Frontiers in Life Science,* 6(3–4), 107–117.

Ren, X., Chen, J.-F., 2020. Caffeine and Parkinson's disease: multiple benefits and emerging mechanisms. *Frontiers in Neuroscience,* 14, 602697.

Reshetnikov, D. V., Ivanov, I.D., Baev, D.S., Rybalova, T. V., Mozhaitsev, E.S., Patrushev, S.S., Vavilin, V.A., Tolstikova, T.G., Shults, E.E., 2022. Design, synthesis and assay of novel methylxanthine–alkynylmethylamine derivatives as acetylcholinesterase inhibitors. *Molecules,* 27(24), 8787.

Ronco, C., Foucault, R., Gillon, E., Bohn, P., Nachon, F., Jean, L., Renard, P.Y., 2011. New huprine derivatives functionalized at position 9 as highly potent acetylcholinesterase inhibitors. *ChemMedChem,* 6(5), 876–888.

Ruggiero, M., Calvello, R., Porro, C., Messina, G., Cianciulli, A., Panaro, M.A., 2022. Neurodegenerative diseases: can caffeine be a powerful ally to weaken neuroinflammation? *International Journal of Molecular Sciences*, 23(21), 12958.

Saeed, A., Mahesar, P.A., Zaib, S., Khan, M.S., Matin, A., Shahid, M., Iqbal, J., 2014. Synthesis, cytotoxicity and molecular modelling studies of new phenylcinnamide derivatives as potent inhibitors of cholinesterases. *European Journal of Medicinal Chemistry*, 78(2014), 43–53.

Santos, G.F. Dos, Takahashi, J.A., 2017. A new acetylcholinesterase inhibitor from green glycosylation of trachyloban-19-oic acid by Mucor plumbeus. *Anais da Academia Brasileira de Ciencias,* 89(3), 1961–1969.

Sinha, S.K., Shrivastava, S.K., 2013. Synthesis, evaluation and molecular dynamics study of some new 4-aminopyridine semicarbazones as an antiamnesic and cognition enhancing agents. *Bioorganic and Medicinal Chemistry,* 21(17), 5451–5460.

Tira, R., Viola, G., Barracchia, C.G., Parolini, F., Munari, F., Capaldi, S., Assfalg, M., D'Onofrio, M., 2023. Espresso coffee mitigates the aggregation and condensation of Alzheimer's associated tau protein. *Journal of Agricultural and Food Chemistry*, 71(30), 11429–11441.

Waskitha, S.S.W., Istyastono, E.P., Riswanto, F.D.O., 2023. Molecular docking study of caffeic acid as acetylcholinesterase inhibitor. *Journal of Food and Pharmaceutical Sciences,* 11(3), 867–873.

Windah, A.L.L., Istyastono, E.P., 2024. Computational studies of donepezil and acetylcholinesterase molecular dynamics interactions. *Jurnal Farmasi Sains dan Komunitas*, 21(1), 91–99.

Zhang, X., He, X., Chen, Q., Lu, J., Rapposelli, S., Pi, R., 2018. A review on the hybrids of hydroxycinnamic acid as multi-target-directed ligands against Alzheimer's disease. *Bioorganic and Medicinal Chemistry*, 26(3), 543–550.

Ziemianin, A., Ronco, C., Dolé, R., Jean, L., Renard, P.Y., Lange, C.M., 2012. Screening of new huprines-inhibitors of acetylcholinesterases by electrospray ionization ion trap mass spectrometry. *Journal of Pharmaceutical and Biomedical Analysis*, 70, 1–5.